U O W

Energy Release and Failure Model of Coal Samples

-Laboratory Test and Numerical Modelling

Dr. Ting Ren

Xiaohan Yang & Lihai Tan

University of Wollongong

UNIVERSITY
OF WOLLONGONG
AUSTRALIA

Content

1. Introduction

2. Energy Analysis

3. Numerical Analysis

4. Current Work

5. Conclusions

Introduction

Coal Bursts in Australia

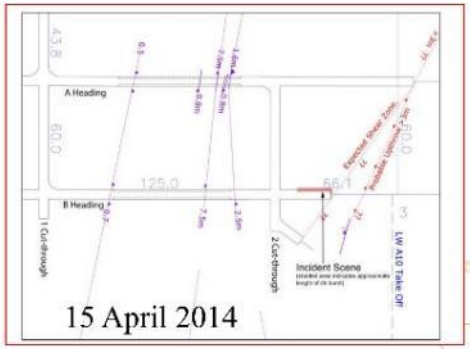

19 August 2016

Coal burst occurred on LW B2 lonwall face. Barraba Fault located on the south-west corner of longwall face.

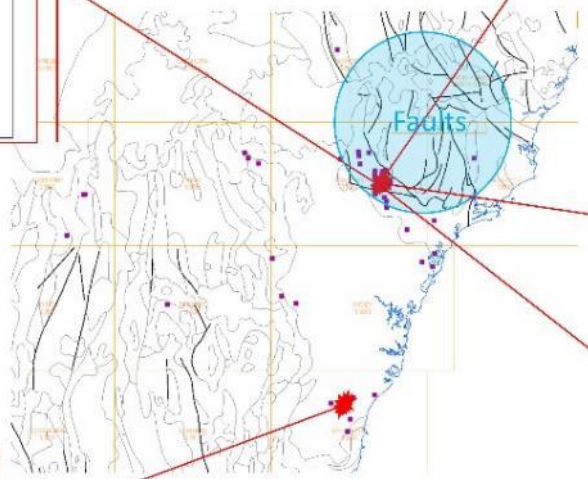

2 February 2018

Coal burst occurred on LW B4 longwall face.

17 May 2018

Coal burst occurred on longwall face.

27 May 2018

Coal burst occurred in the roadway at the development panel.

Structural Geology of Coal Burst Sites

Energy Analysis

Static and Dynamic Load Superposition Theory

Coal burst will occur when the sum of static and dynamic load exceeds the minimum load required for coal burst formation. The energy released during coal burst is provided by static load and dynamic load.

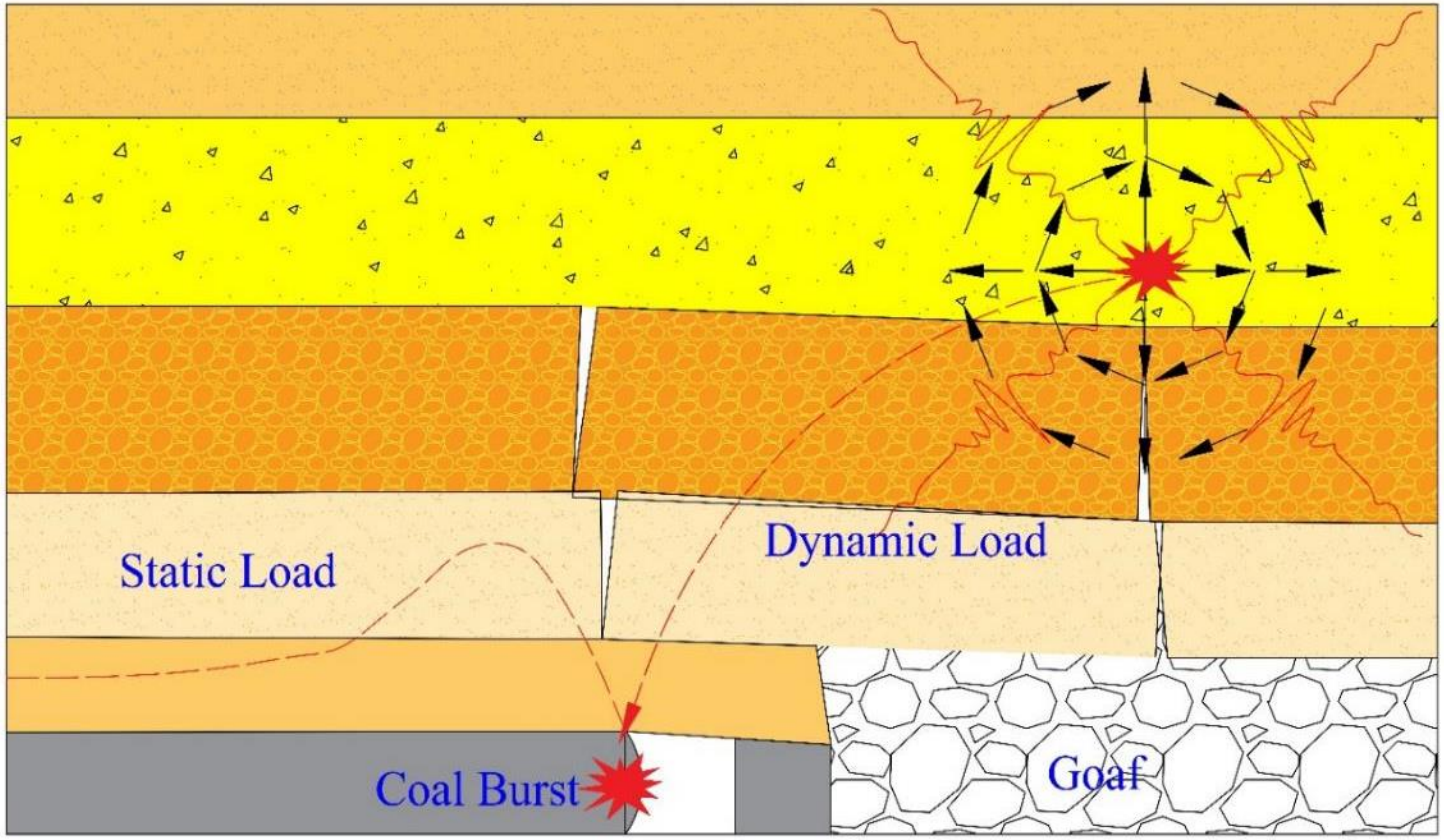

Coal Burst Induced by Static and Dynamic Load superposition (Dou et al)

Energy Analysis

Energy Sources of Coal Bursts in Australia

Elastic energy accumulation resulted from high mining depth and complicated geological structure is the major contribution of energy sources of coal burst.

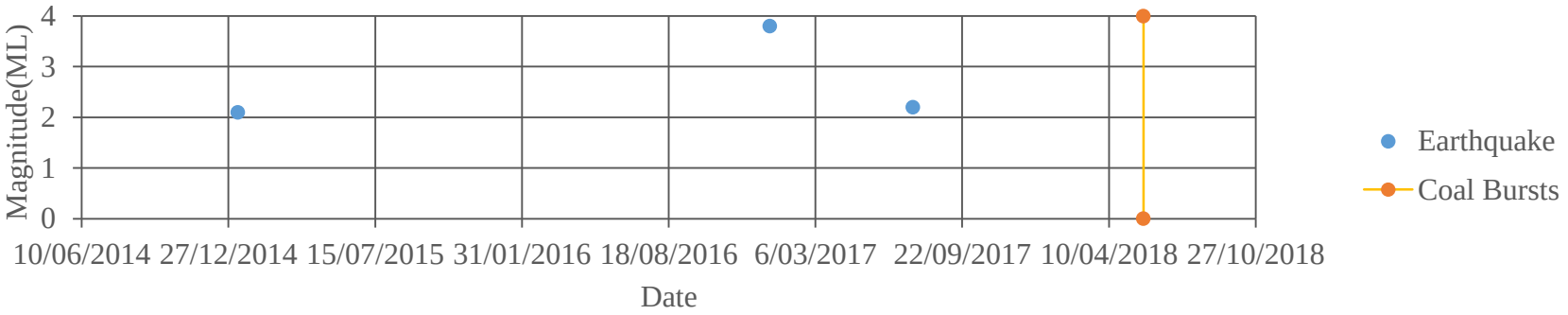

Coal Burst of Coal Mine A

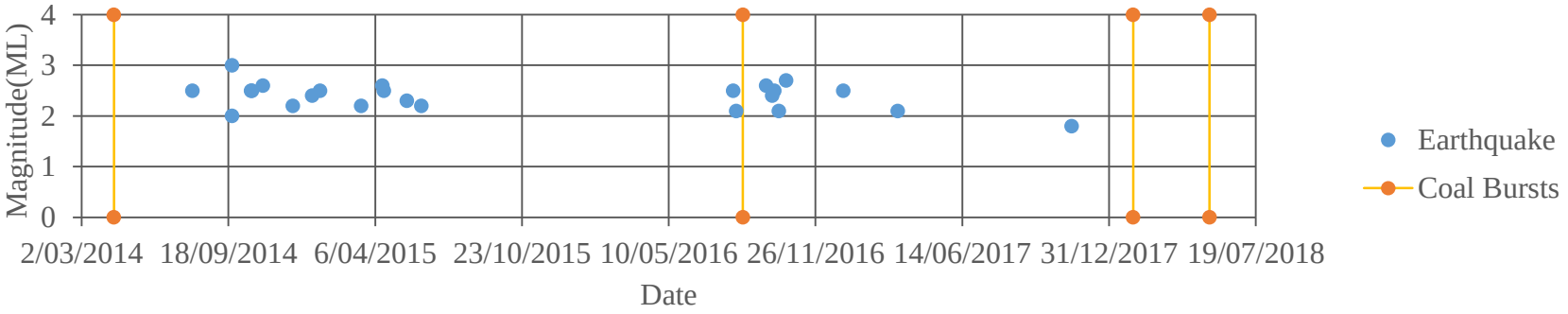

Coal Burst of Coal Mine B

Energy Analysis

Energy Dissipation Analysis

$$E_{plastic} + E_{elastic} = E_{total}$$

$$E_{elastic} = E_{crushing} + E_{kinetic} + E_{residual}$$

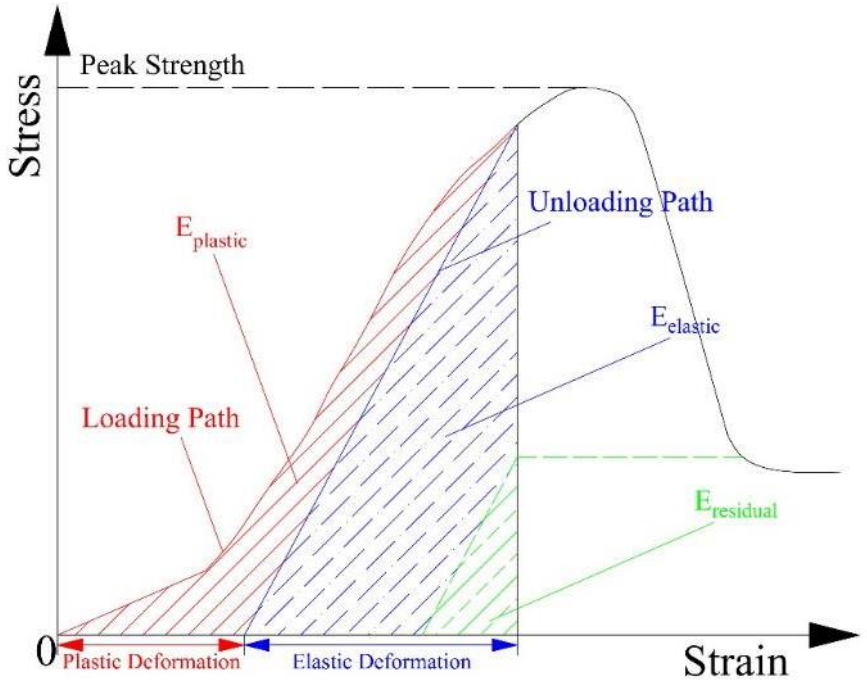

Schematic Diagram of Energy Accumulation before Peak Strength

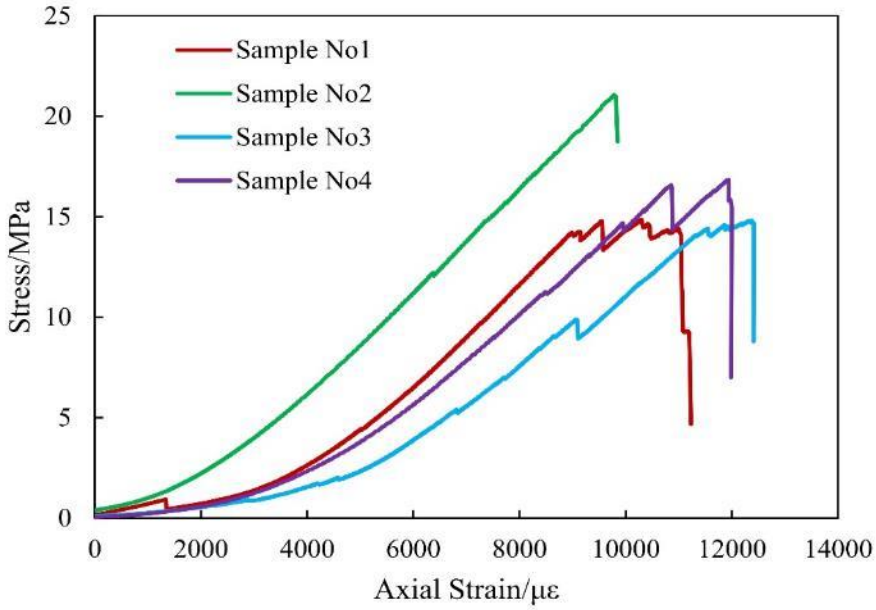

Stress versus Strain Curve of Coal Samples

Energy Analysis

Coal Burst Propensity Index

Coal burst propensity index method is an effective way to evaluate the burst risk of coal mines. Further tests with different coal seams are required in order to develop specific coal burst propensity classification method for Australian coal seams.

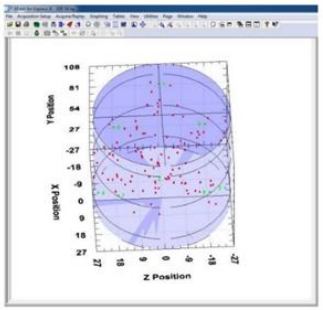

Locating of AE Sources


Loading Machine


Violent Failure

Risk Classification Form

Type		I	II	III	IV
Burst Propensity		None	Low	Moderate	High
Index	DT/ms	DT > 10000	1000 < DT ≤ 10000	500 < DT ≤ 1000	DT ≤ 500
	K_E	$K_E < 2$	$2 \le K_E < 3.5$	$3.5 \le K_E < 5$	$K_E \ge 5$
	W_{ET}	$W_{ET} < 2$	$2 \le W_{ET} < 3.5$	$3.5 \le W_{ET} < 5$	$W_{ET} \ge 5$
	R_C/Mpa	$R_C < 5$	$5 \le R_C < 10$	$10 \le R_C < 15$	$R_C \ge 15$

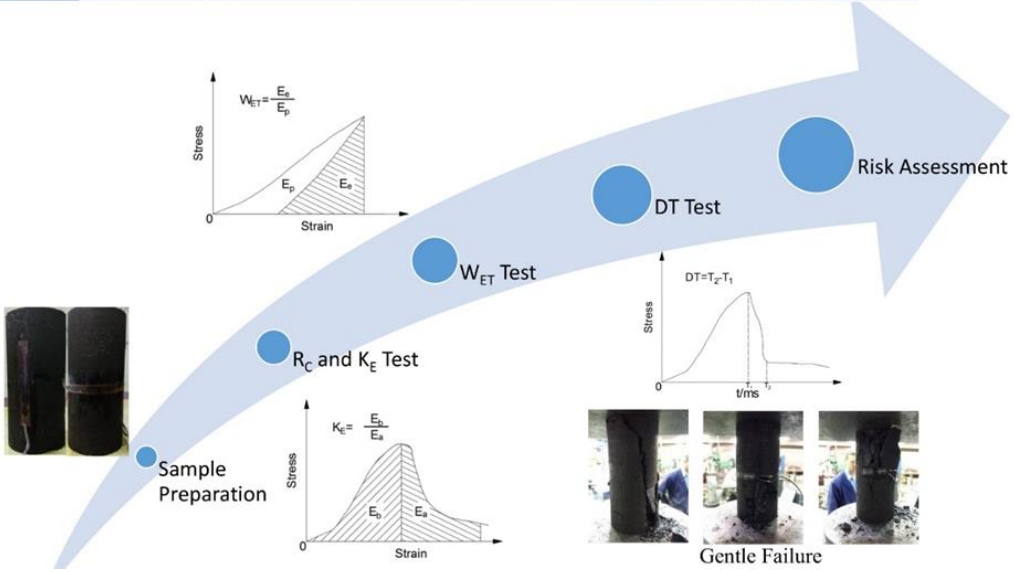

Gentle Failure

Coal Burst Propensity Index Test

Energy Analysis

Coal Burst Propensity Index

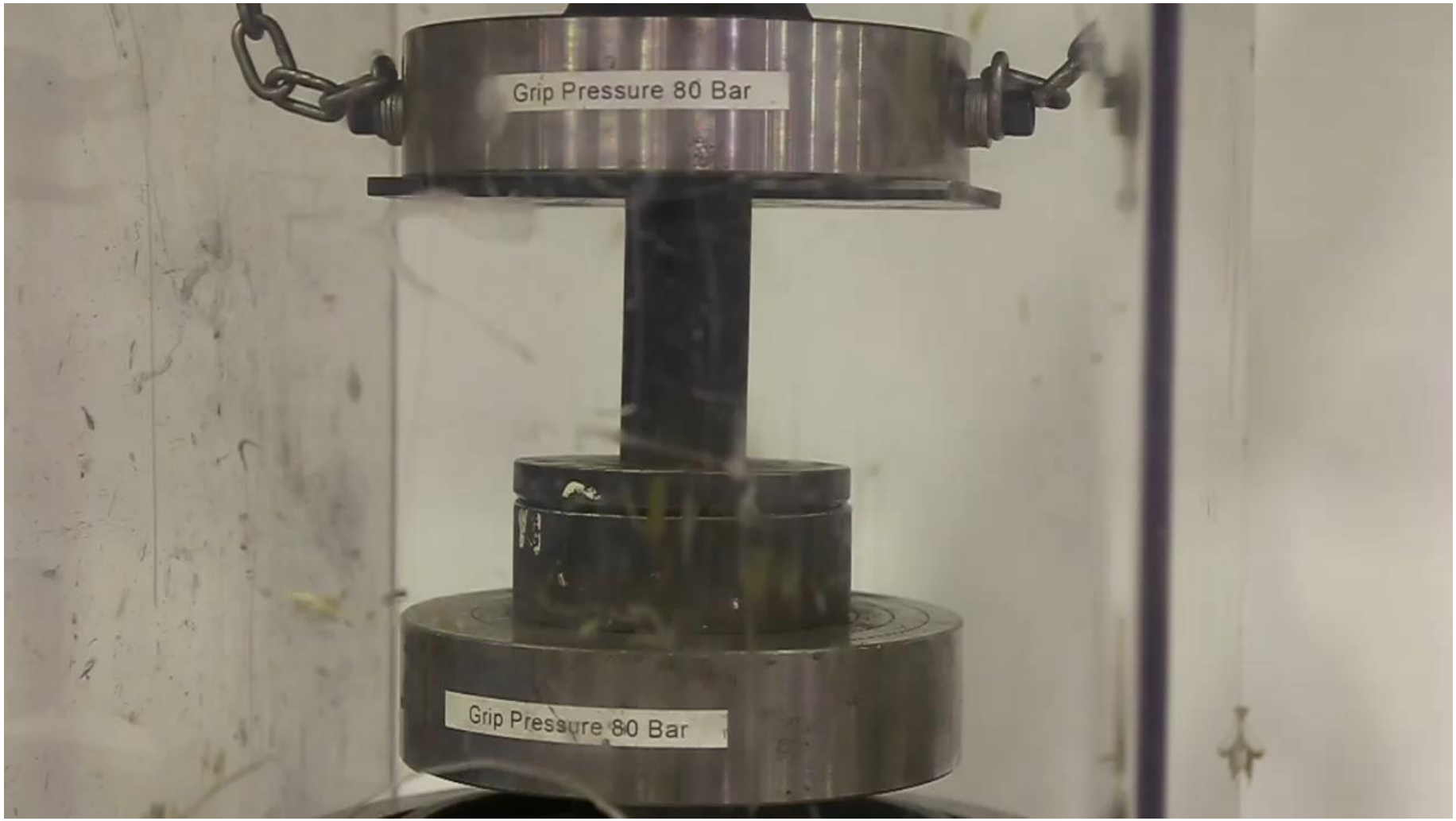

Energy Analysis

Kinetic Energy Estimation

$$E_{elastic} = \frac{V}{2E_0}[\sigma_1^2 + \sigma_2^2 + \sigma_3^2 - 2\mu(\sigma_1\sigma_2 + \sigma_2\sigma_3 + \sigma_3\sigma_1)]$$

$$E_{kinetic} \cong E_{elastic} - E_{crushing}$$

$$F(d) = (\frac{d}{d_{max}})^{(3-n)}$$

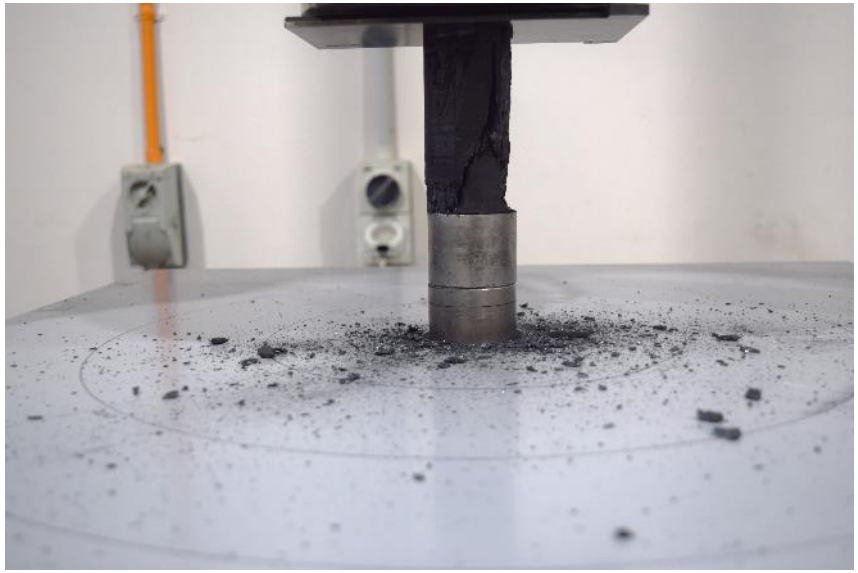

Coal Ejection Test

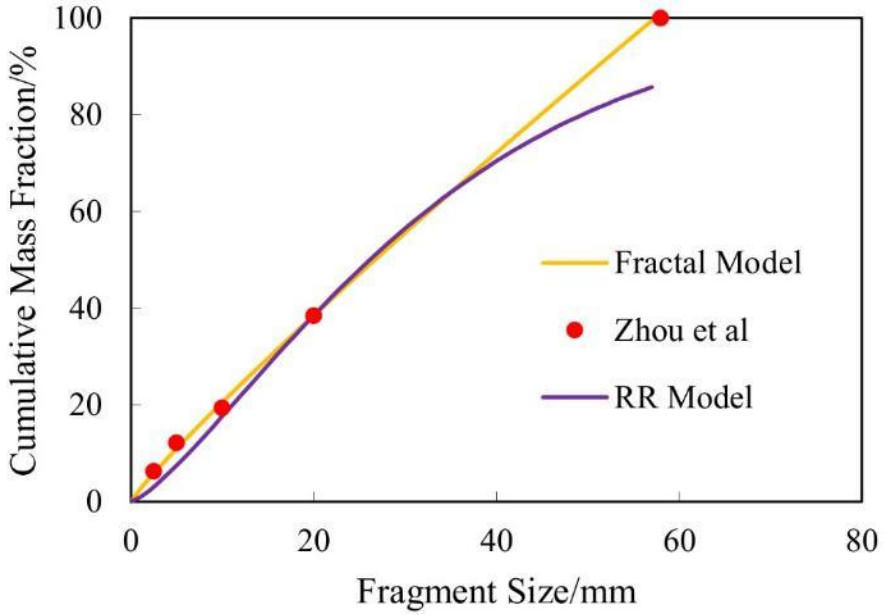

Fitting Functions of Fragment Size Distribution

Energy Analysis

Kinetic Energy Estimation

The estimated kinetic energy carried by ejected coal is between 16.24 and 20.35 MJ. Considering the total mass of ejected coal, the average initial speed of ejected coal particles ranges from 24.98 to 27.96 m/s.

Value of Main Parameters for Crushing Energy Estimation

Mining Depth	Stress Concentration Factor	Vertical Stress	Shape Factor	Density	Volume of Ejected Coal	Weight of All Fragments	Rittinger Constant
555 m	1.75-2.87	24.28-39.82 MPa	1.5	1.37 g/cm2	38 m^3	52.06 t	178.84 - 242.06

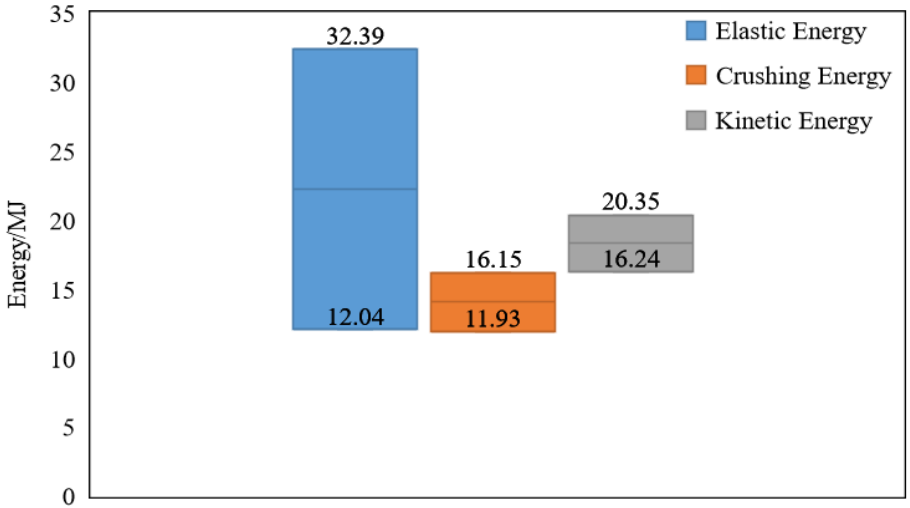

Estimated Value of Kinetic Energy of Sidewall Burst

Numerical Analysis

-water effect on coal burst of pillar under geo-stress

Numerical model

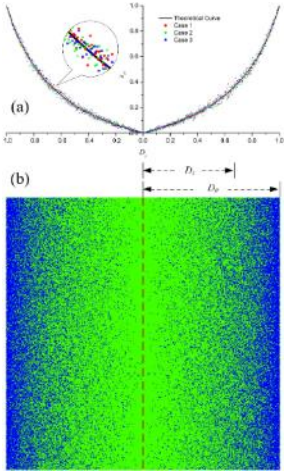

The water distribution curve and numerical model (sc=0.3); the blue patterns represent water-weakened contacts and the green patterns represent normal contacts.

Sectional saturation coefficient s_{ci}

$$s_{ci} = m - \frac{m(1-m)}{D_r - m} \qquad m < 0 \; or \; m \geq 1$$

Overall water saturation coefficient s_c

$$s_c = 2\int_0^1 D_r \times s_{ci}\, dD_r = \mathrm{m} + 2m(1-m)\left[1 + (1-\mathrm{m})\ln\left(\frac{m}{m-1}\right)\right]$$

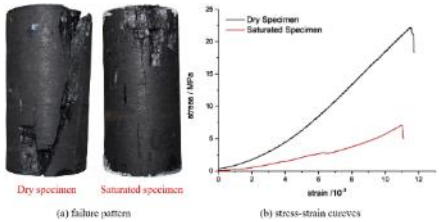

Comparison between experimental results of dry specimen and saturated specimen under uniaxial compression

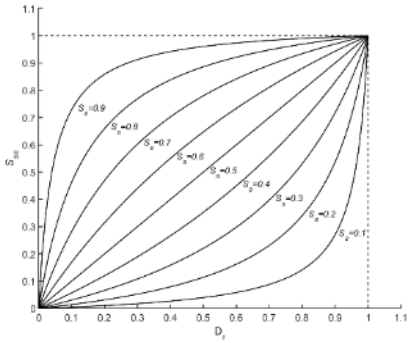

The relationship between saturation degree and distance ratio: (a) saturation distribution; (b) evaporation distribution

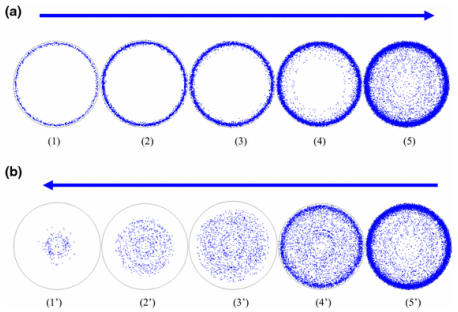

Nuclear magnetic resonance (NMR)-images of sandstone disk with different water contents: a saturation process; b drying process (Zhou, 2016)

NMR-images of sandstone disk in saturation condition

Numerical Analysis

Experiment preparation

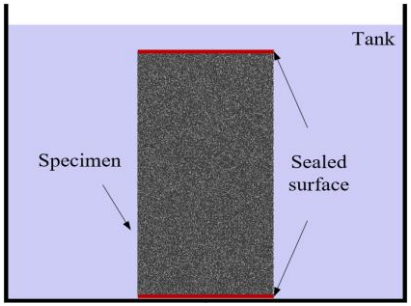

Specimen No.	Group	Estimated saturation coefficient	Actual water content (%)	Length /mm	Diameter /mm
D-1			0.0	108.24	54.02
D-2	1	0	0.0	108.03	53.83
D-3			0.0	107.94	53.74
M-1			0.47	108.15	53.89
M-2	2	0.3	0.62	108.18	53.92
M-3			0.58	108.32	53.61
H-1			1.24	107.87	53.87
H-2	3	0.7	1.15	108.26	53.93
H-3			1.29	108.07	53.75
S-1			1.66	108.13	53.82
S-2	4	1.0	1.67	108.19	53.64
S-3			1.88	108.24	53.71

Schematic of soaking test for cylinder coal specimens and parameters of specimens for compression tests

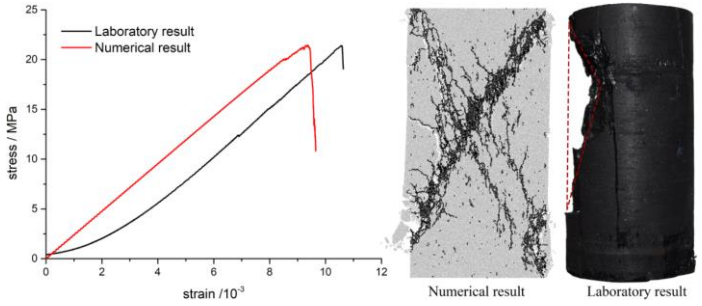

Comparison between numerical and experimental results of dry specimen under uniaxial compression

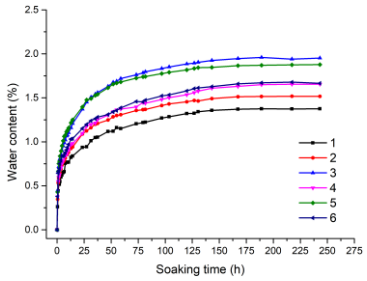

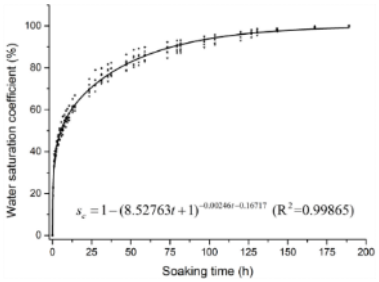

Variation of water content and water saturation coefficient with time for coal specimens

Mechanical properties of intact specimen in laboratory experiment and PFC numerical simulation

Mechanical properties	Experimental result	Numerical result	Deviation
Peak stress /MPa	21.41	21.45	0.19%
Young's modulus /GPa	2.43	2.39	1.65%
Failure strain /10^{-3}	10.57	9.36	11.45%

Numerical Analysis

Parameter calibration

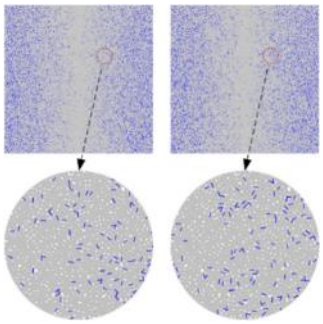

Comparison between two numerical models with the same saturation coefficient

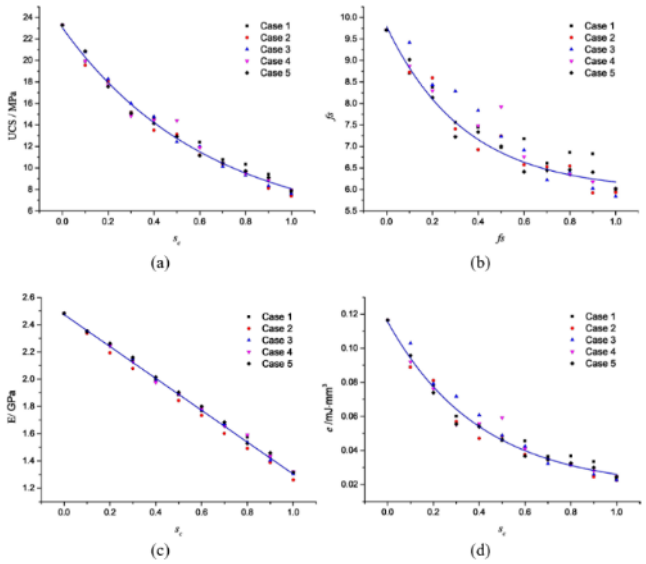

Relationships between water saturation coefficient and mechanical properties in numerical simulations: (a) UCS; (b) Failure strain; (c)Young's modulus; (e) Strain energy per unit volume

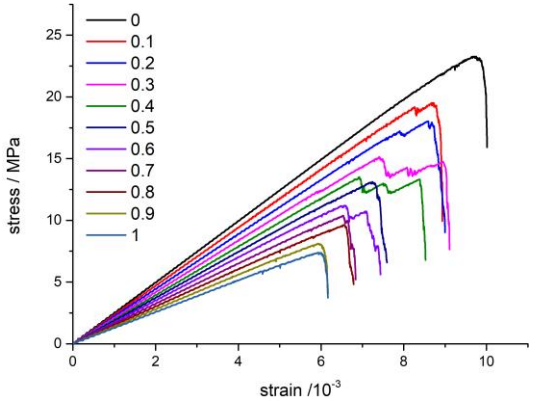

Stress-strain curves for specimens with different saturation coefficients in case 2

The fitting functions between mechanical properties and water saturation coefficient for simulation results

Mechanical properties	Fitting function	R^2
UCS σ_c	$\sigma_c = 4.142 + 18.910e^{-1.573s_c}$	0.9961
Failure strain fs	$fs = 5.965 + 3.825e^{-2.905s_c}$	0.9770
Young's modulus E	$E = 2.475 - 1.171s_c$	0.9982
Absorbed energy per unit volume e	$e = 0.037 + 0.067e^{-2.650s_c}$	0.9997

Numerical Analysis

Numerical simulation

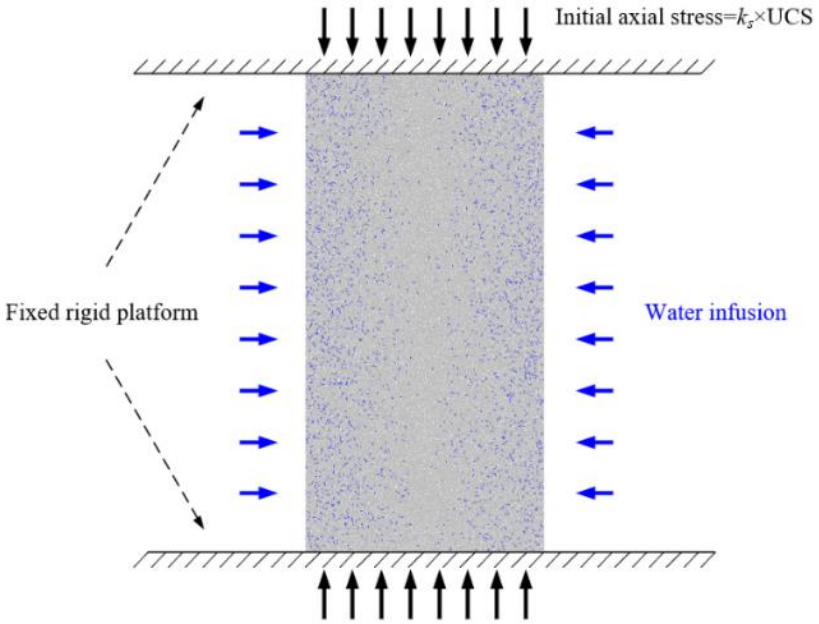

Sketch of the numerical experiment

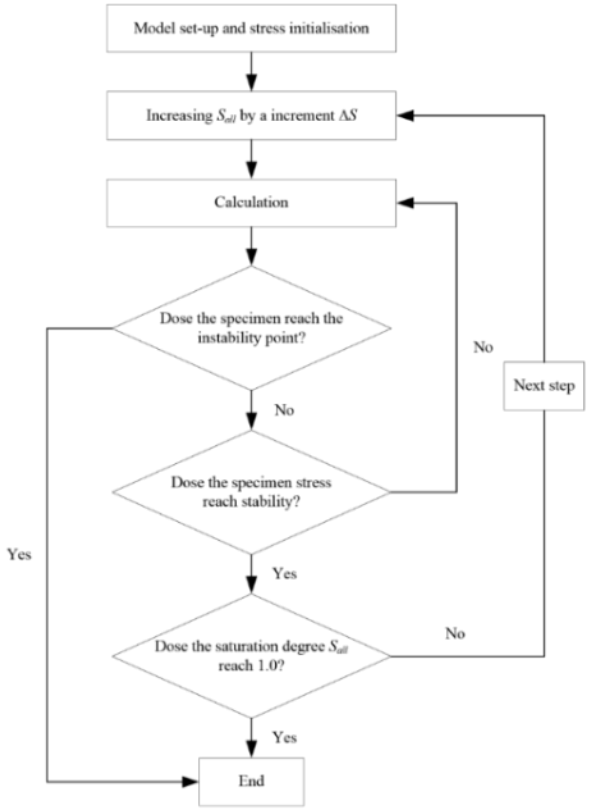

Flow chart for the simulation procedure

Numerical Analysis

Stress evolution

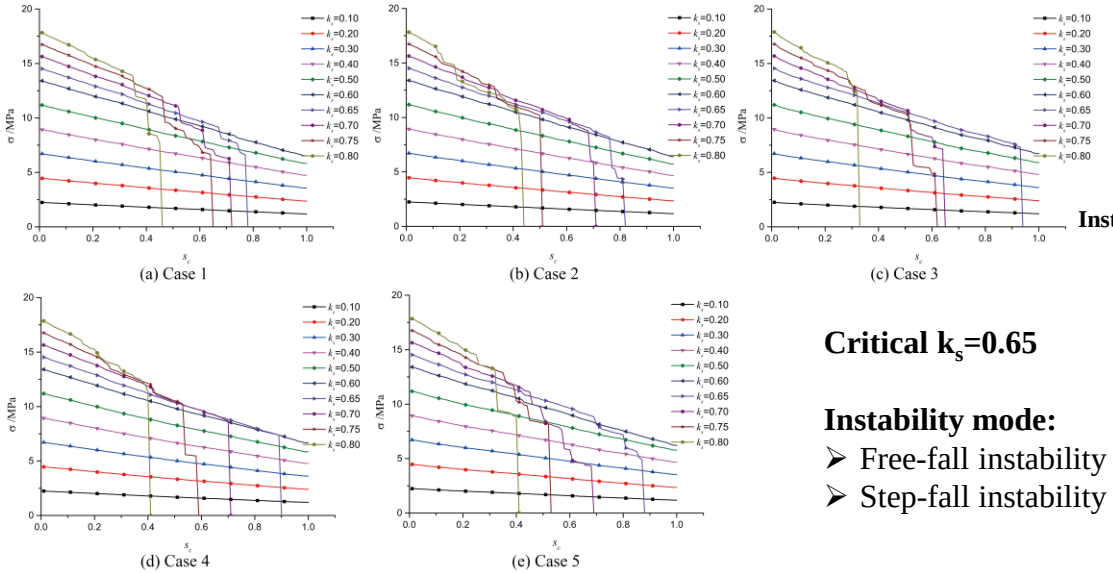

Stress evolution with the increase of water saturation coefficient s_r under different initial stress conditions

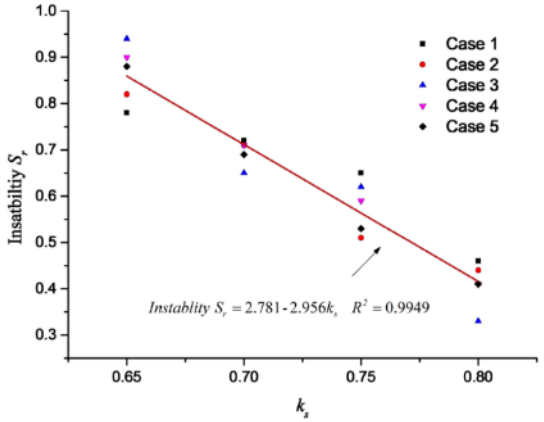

Instability water saturation coefficient for specimens in high-stress conditions

Critical k_s=0.65

Instability mode:

- Free-fall instability
- Step-fall instability

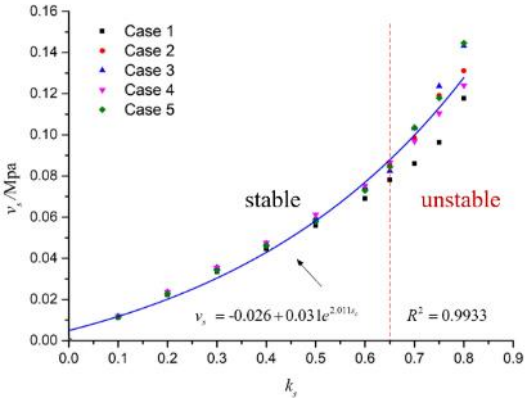

v_s evolution curves with k_s increasing

Stress energy releasing rate vs: the decrement of axial stress when the water saturation coefficient increased 1%

Numerical Analysis

Energy evolution

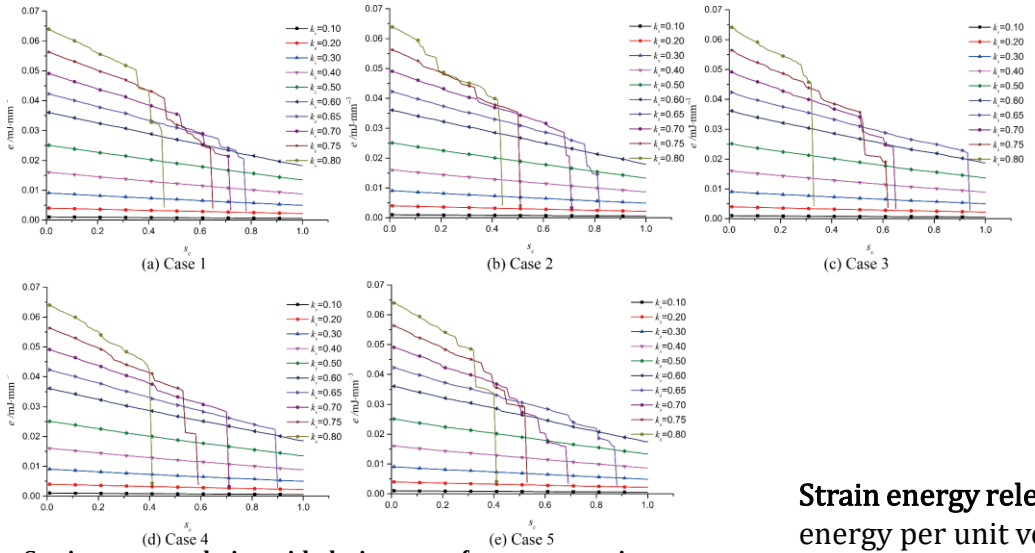

Strain energy evolution with the increase of water saturation coefficient under different initial stress conditions

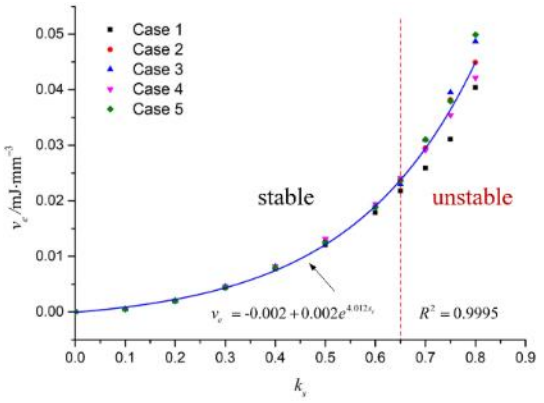

ve evolution curves with ks increasing

Strain energy releasing rate v_e: the decrement of released strain energy per unit volume when the water saturation increased 1%

Strain energy per unit volume e

$$e = \frac{W}{V}$$

W is the total work done by the testing system before the instability point of a specimen, V is the volume of the specimen

Initial stress coefficient:

65%~80% UCS: Lower instability point and higher coal burst risk.

40%~65% UCS: Water infusion is an effective approach to reduce coal burst risk as having been reported by many literatures.

≤40% UCS: Water has limited effect on releasing stress and energy for coal.

Numerical Analysis

Failure mode

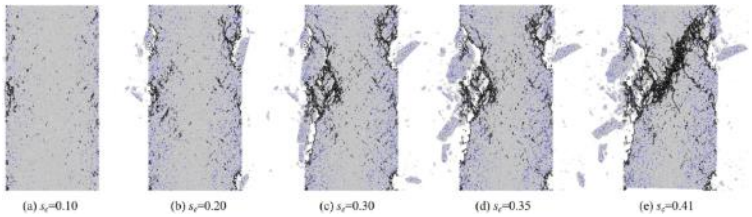

Failure evolution of specimen in Case 5, ks=0.8

- Similar failure patterns
- Splitting failure in water-rich area
- Shear-dominated failure

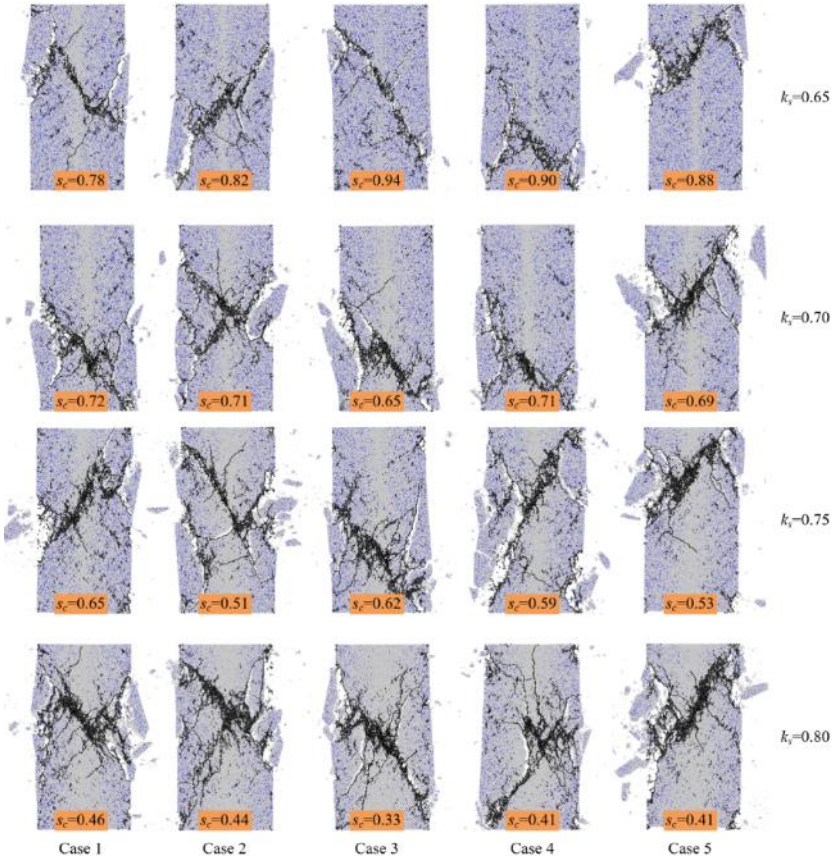

Final failure patterns of all damaged specimens

Current Work

Numerical Modelling of Dynamic Load

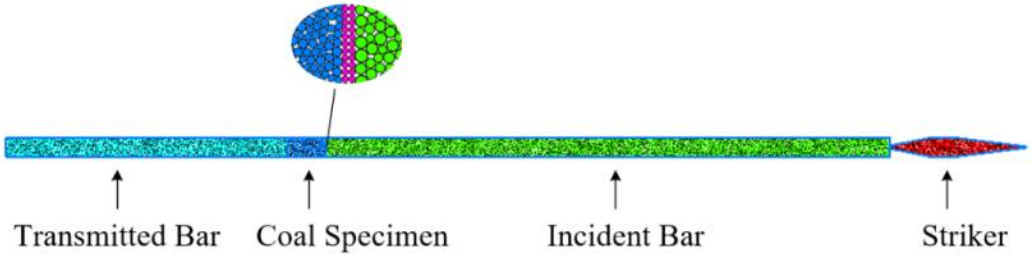

Numerical model of SHPB test system

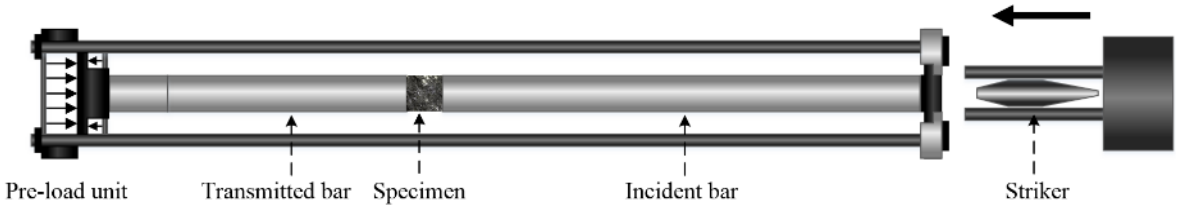

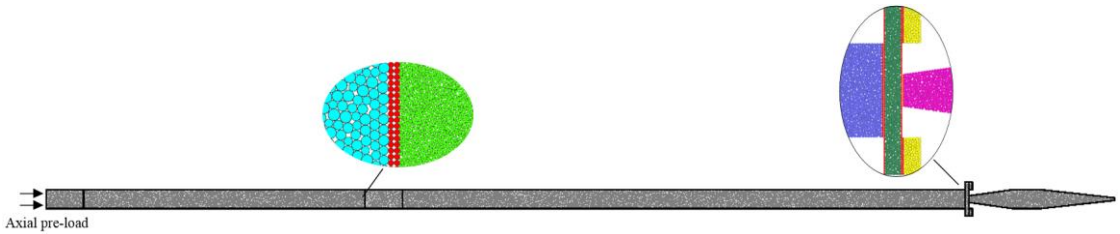

Numerical model of Pre-load SHPB test system

Drop hammer test system

Current Work

Protective Structure on CM

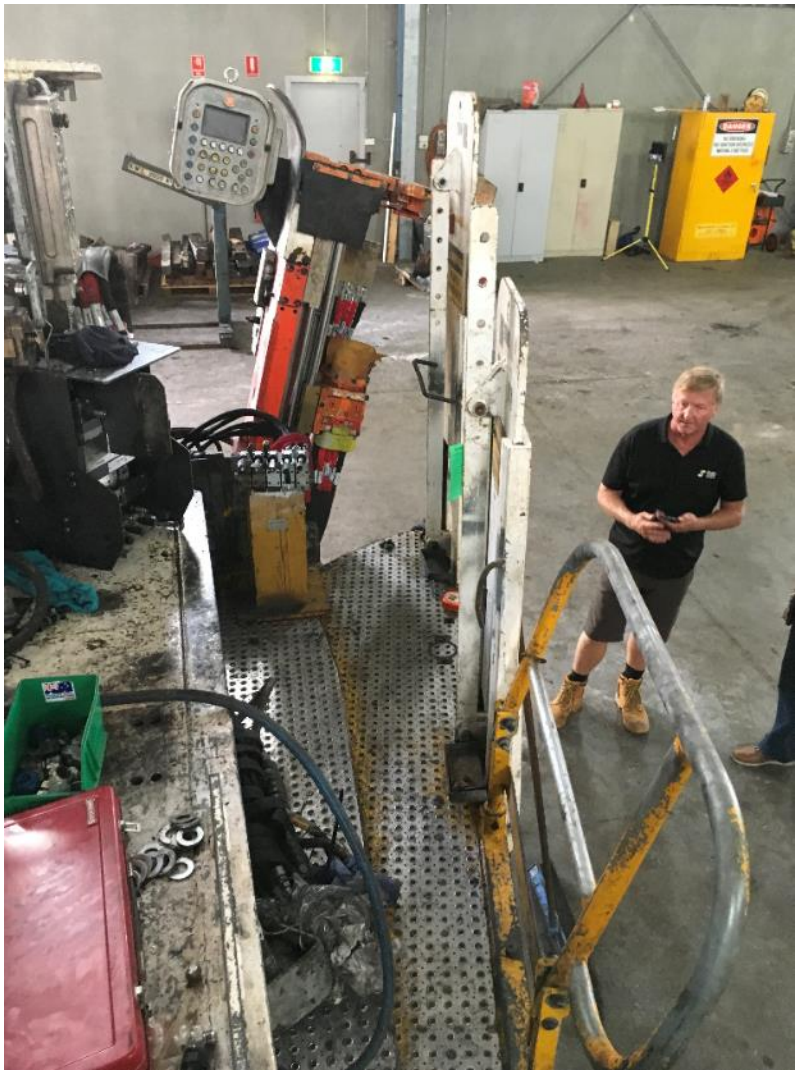

Conclusions

Energy Analysis

1. The main energy source of coal burst is provided by static load.

2. Coal burst propensity index can evaluate the coal burst risk by reflecting the energy accumulation and dissipation behavior.

3. The average ejection velocity of coal particles from roadway sidewall can reach 24.98-27.96 m/s.

Numerical modeling of pillar instability

1. Instability

   Free-fall instability : stress and energy decreased linearly and stably and then overall instability appeared suddenly.

   Step-fall instability : several times of stress and energy drop and had been damaged obviously before the final instability.

2. The axial stress and strain energy within the specimens are more sensitive to water under a higher initial axial stress condition.

3. The stress releasing rate v_s and energy releasing rate v_e are suggested to be an effective index to assess the stability and of pillar.

Questions?